GEOLOGY AND Cr-PGE MINERALIZATION OF THE BIRCH LAKE AREA, SOUTH KAWISHIWI INTRUSION, DULUTH COMPLEX

By

S. Hauck and M. Severson[1]
E. Ripley[2]
S. Goldberg[3]
T. Alapieti[4]

December 1997

Technical Report
NRRI/TR-97/13

Direct and Indirect Funding Provided By:
Minnesota Mining and Mineral Resources Research Institute, Univ. of Minnesota, Minneapolis, Minnesota
Natural Resources Research Institute, Univ. of Minnesota, Duluth, Minnesota
Institute of Electron Optics and Department of Geology, Univ. of Oulu, Oulu, Finland
Department of Geology, Indiana Univ., Bloomington, Indiana
Department of Geology, Univ. of North Carolina, Chapel Hill, North Carolina

Project No. 5693201

[1]Natural Resources Research Institute
University of Minnesota, Duluth
Duluth, Minnesota

[2]Department of Geology
Indiana University
Bloomington, Indiana

[3]Department of Geology
University of North Carolina
Chapel Hill, North Carolina

[4]Department of Geology
University of Oulu
Oulu, Finland

PREFACE

This report is a summary of geochemical data collected during 1993-1994. The report is meant primarily to make the data more readily available. Future reports will further address the origin of pre-Complex footwall sills and the PGE-Cr mineralization in the Birch Lake area.

LIST OF FIGURES

Figure 1. Location map showing Birch Lake study area along the western margin of the Duluth Complex 20

Figure 2. Diagram of PGE-Cr-Cu-Ni-S values in Du-15 from 2,400 ft. to 2,435 ft. 21

Figure 3. Schematic cross-section of the igneous stratigraphy in the South Kawishiwi Intrusion (from Severson, 1994) 22

Figure 4. AFM (Jensen, 1976) diagram showing the dual differentiation trends in the troctolitic rocks and the geochemical differences between the Logan-type and Cr-rich sills 23

Figure 5. Fe_2O_3 vs. MgO diagram illustrating the dual differentiation trends within the troctolitic rocks of the U3 Unit 23

Figure 6. Cu/Pd vs. Pd diagram of Barnes et al. (1993) showing the enrichment of the U3 Unit compared to other South Kawishiwi unit samples 24

Figure 7. Generalized stratigraphic section of the Virginia Formation and underlying Biwabik Iron Formation showing approximate location of Cr-rich and Logan-type sills (after Gundersen and Schwartz, 1962, and Severson, 1994) 25

Figure 8. Normalized rare-earth element diagram illustrating the REE differences between the Logan-type and Cr-rich sills 26

Figure 9. Mg# vs. Al_2O_3 illustrating the geochemical differences between the Logan-type, Cr-rich, and Pigeon Point sills and samples from the Crystal Lake Intrusion 27

Figure 10. Du-15 downhole mineral chemistry for olivine, pyroxene, and plagioclase with geological units of Severson (1994) 28

Figure 11. Downhole geochemical changes for Du-15 (top half) wedge D15-W1 (bottom half) showing changes in major and trace element and base metal chemistry using geology of Severson (1994) 29

Figure 12. δD vs. $\delta^{18}O$ for unmetamorphosed and metamorphosed pelitic rocks of the Virginia Formation and for igneous rocks of the Partridge River and South Kawishiwi intrusions 30

Figure 13. εNd vs. εSr at T=1,100 (after Seifert et al., 1992) for various Midcontinent Rift System intrusive and extrusive rocks 31

Figure 14. A. Linear distribution of massive sulfides, disseminated sulfides, and copper-rich veins in the Giants Range Batholith footwall; B. Linear distribution of late-stage granitoid and pyroxenitic rocks in the pyroxenitic rocks in the Duluth Complex (after Severson, 1994) 32

LIST OF TABLES

Table 1. List of samples analyzed by various geochemical methods 11

Table 2. PGE, Cu, Ni, Au, Ag, and Cr analyses from the Birch Lake area, South Kawishiwi Intrusion, Duluth Complex 13

Table 3. Stable isotope data, Birch Lake area, South Kawishiwi Intrusion, Duluth Complex 15

Table 4a. Sm-Nd analyses from the Birch Lake area, South Kawishiwi Intrusion, Duluth Complex 17

Table 4b. Rb-Sr analyses from the Birch Lake area, South Kawishiwi Intrusion, Duluth Complex 18

Table 4c. U-Pb analyses from the Birch Lake area, South Kawishiwi Intrusion, Duluth Complex 19

SUMMARY

Platinum-group element (PGE) mineralization (>8 ppm Pt+Pd over 10 ft.) in the Birch Lake area (Fig. 1) was first recognized in DDH Du-15 associated with chrome spinels (Cr hercynite) and massive oxide (magnetite>ilmenite) mineralization (Fig. 2; Sabelin, 1985, 1987; Sabelin and Iwasaki, 1985, 1986; Sabelin et al., 1986). Additional drilling in the Birch Lake area intersected both PGE and chromium mineralized zones (some were coincident); however, the PGE-enriched zones were not always associated with massive oxide horizons (Severson, 1994). Recent stratigraphic correlation (Fig. 3) of the basal igneous units in the Birch Lake area drill holes showed that the PGE and chromium mineralization were located primarily in the U3 ultramafic unit (U3 Unit) and also in the basal portion of the overlying PEG Unit. Severson (1994) showed that the average PGE content of the U3 Unit is higher than all other units in the South Kawishiwi Intrusion.

The U3 Unit consists of interlayered melatroctolite (picrite), oxide melatroctolite, massive oxide (magnetite>ilmenite), and minor troctolite. The U3 Unit also contains recognizable inclusions of Biwabik Iron-Formation (BIF). Severson (1994) has suggested that the more pyroxenitic units within the U3 Unit are actually recrystallized BIF. Overlying the U3 Unit is the PEG Unit that is largely comprised of pegmatitic troctolitic rock intermixed with lesser amounts of medium- to coarse-grained troctolitic rock. Beneath the U3 Unit are the troctolitic and noritic rocks of the Basal Augite Troctolite-Norite Unit (BAN; Fig. 3). The footwall in the Birch Lake area consists of contact metamorphosed granitic rocks of the Archean Giants Range Batholith, which in the area of PGE-Cr mineralization also contain disseminated and massive sulfide mineralization (cp>po).

Geochemical diagrams (Figs. 4-5; Table 1 shows samples analyzed) illustrate two different trends in the U3 Unit rocks. On an MgO vs. TFe_2O_3 diagram (Fig. 5), troctolitic rocks of both the PEG and U3 units fall on a trend of slightly decreasing TFe_2O_3 (also TiO_2, V, and Al_2O_3) with decreasing MgO. Another trend defines the iron-rich rocks, which show sharply increasing TFe_2O_3

with decreasing MgO. SiO_2, CaO, and Na_2O decrease with decreasing MgO. PGE data (Table 2), when plotted on petrochemical diagrams (Fig. 6) of Barnes et al. (1993), indicate that the PGEs have a mantle origin and have not been remobilized a great distance by later hydrothermal fluids from their original emplacement site.

Up dip from the Birch Lake area are several pre-Duluth Complex sills that intrude the footwall Virginia Formation and the BIF (Fig. 7; Grout and Broderick, 1919; Gundersen and Schwartz, 1962; Hauck, 1993; Severson, 1994; and Severson and Barnes, 1991). Geochemistry (Figs. 4, 8-9) and Sm-Nd data (Fig. 13) indicate there are two different types of sills, i.e., Logan-type and Cr-rich type. The Logan-type sills have plagioclase phenocrysts locally, and occasionally clinopyroxene phenocrysts, and only intrude the BIF. Severson (1997) reports that the K-Sill in the Allen 7½ minute quadrangle is the farthest western extension of Logan-type sills. The Cr-rich sills are homogeneous and fine-grained and have been identified in both the BIF and Virginia Formation. In the Virginia Formation, the Cr-sills consist of a medium-grained, hornblende-rich (±olivine) core surrounded by a very fine- to fine-grained "rim" termed the MG Unit by Severson et al. (1994, 1996). Both sets of sills have undergone contact metamorphism. CIPW norms indicate the Logan-type sills are quartz normative, and the Cr-rich sills range from olivine to slightly quartz normative. The Cr-rich sills have from 800-2,000 ppm Cr, versus <100 ppm Cr for the Logan-type, and define a differentiation trend on a Mg# vs. Al_2O_3 diagram (0.78 to 0.62; Fig. 9). The Logan-type sills generally have Mg# of ~0.35 and show no differentiation trend (Fig. 9). This same relationship occurs with other elements, e.g., Sc vs. MgO and TiO_2, TFe_2O_3 vs. MgO, etc. The Cr-rich sills are chemically very similar to basalt inclusions in the Serpentine Cu-Ni deposit area, suggesting that the Cr-rich sills represent feeders to upper level basalt flows. In addition, two samples of the Crystal Lake Gabbro (Geul, 1970), which are known to have PGE-Cr mineralization (Cogulu, 1993a-b;

Eckstrand et al., 1989), geochemically plot along with the Cr-rich sills. This comparison suggests that the Cr-rich sills may also be enriched in PGEs.

Textures and mineralogy observed by Severson (1994) in the South Kawishiwi Intrusion suggest the massive oxides, pyroxenites, and related rocks within the U3 Unit may be metasomatized BIF. Muhich (1993) describes the metasomatism of the BIF at its contact with the SKI at Dunka Pit and shows Ti, U, Al, Ca, Na, K, Ba, Rb, Sr, MgO, Cu, and Ni gains in the BIF, while the SKI gained silica and iron. In the BIF, ilmenite, plagioclase, cpx, and opx were formed as a result of the metasomatism. Alapieti (1991) petrographically describes textures (atoll texture of Hulbert and Von Gruenewaldt, 1985) in Du-15 massive oxide samples that could have been formed by the sintering of pre-existing BIF oxides. This texture, referred to as "two rocks in one," consists of round to sintered oxide grains that are poikilitically enclosed in very coarse plagioclase laths. Downhole (Fig. 10; Du-15) mineral chemistry for olivine, pyroxene, and plagioclase compositions clearly defines the top of both the PEG and U3 Units, but also illustrates the wide variation in mineral chemistry within the basal units. These variations support a model of magma contamination through assimilation of footwall rocks for the basal units. Similar relationships are apparent in downhole geochemical plots as well (Fig. 11).

The high Cr contents present within certain massive oxide portions of the U3 Unit were, at the beginning of this investigation, thought to be related to metasomatism of inclusions of BIF that had been previously intruded by a Cr-rich sill. In this manner, the sill within the BIF inclusion could have provided Cr, and possibly PGEs, to the metasomatized BIF that eventually produced the massive oxides of the U3 Unit. However, many of the initial thoughts about an origin of this type are not fully substantiated by the data presented herein. Some remobilization of PGEs by later Cl-rich fluids is clearly indicated. Samples with high PGEs can also have high chlorine contents (847-7,840 ppm), and secondary chlorine blooms are visible on the same surfaces of the drill core. The

origin of the Cl-rich fluids may relate to either an enrichment in a magmatic differentiate and/or to an older footwall source beneath the Complex. Secondary chlorides (1,150 ppm Cl) have been identified in Submember C of the footwall BIF (see Fig. 7) in several drill holes to the south and southwest of Birch Lake (Severson, 1994; this study).

Oxygen (4-6 ‰) and sulfur (1.8-9.6 ‰) isotopes (Table 3) from the Birch Lake area exhibit a typical wide variation as observed in the Babbitt and Dunka Road Cu-Ni deposits (Andrews, 1987; Andrews and Ripley, 1989; Ripley and Al-Jassar, 1987; Ripley and Taib, 1989; Ripley et. al., 1992, 1993). The oxide-rich rocks generally have lighter oxygen isotope values (1.8-3.3 ‰) due to fractionation of the lighter isotope into the oxides. However, the sulfur and oxygen isotopes from the Logan-type and Cr-rich sills exhibit heavy contamination (δS^{34} >10.8 ‰ and δO^{18} 10.5-16.6 ‰, respectively). A hydrogen-oxygen isotope diagram indicates that the Birch Lake rocks have not been subjected to as many post-crystallization alteration (fluids) events compared to the Babbitt/Minnamax Cu-Ni deposit area, and also that meteoric waters were involved in the hydrothermal alteration (Fig. 12).

Sm-Nd, Rb-Sr, and Pb-Pb isotopes (Table 4a-c) indicate strong crustal contamination of the U3 Unit rocks. In DDH D15-W1 (wedge off of Du-15) the gNd values decrease downhole toward the footwall over 130 ft. from -8.97 to -21.52 (Fig. 13). The gNd values at the bottom of the drill hole are in the same range as the contact metamorphosed BIF in the footwall near Birch Lake (-17.87 to -22.69). The gNd for both sets of sills fall in the range of -7.78 to -10.12, which is similar to the values near the top of the U3 Unit. The gNd values calculated at 1,100 Ma for the Birch Lake rocks and sills are similar to other values observed in the rift (Nicholson and Shirey, 1990 and references therein).

The plotted data in Figure 13 (gNd and gSr at T=1,100; data in Table 4a) illustrates the effects of crustal contamination with increasing depth, especially in the samples from drill hole D15-

W1. It is interesting to note that the top two samples from D15-W1 plot in the continental flood basalt field, rather than within the field that defines extrusive rocks of the Midcontinent Rift System. This relationship suggests that these two samples (the second sample is from a massive oxide) are the least contaminated, if at all. Another sample, from drill hole BL-89-2, also plots within the continental flood basalt field. Overall, three samples from the top of the U3 Unit exhibit pristine values with little to no contamination. This relationship contradicts empirical data that suggests that all the massive oxide zones of the U3 Unit are related to assimilated and melted BIF inclusions. Perhaps some of the massive oxides are related to magmatic processes (very top of the U3 Unit); whereas other massive oxide horizons at depth are related to assimilated BIF inclusions. The lowermost sample from D15-W1 supports the latter. It is a pyroxenite that was originally interpreted by Severson (1994) as BIF—perhaps equivalent to submember P (see Fig. 7). δO^{18}-gNd data for this sample supports this correlation.

In summary, the geochemical, isotope, and logging data support a multiple and complex origin for the Birch Lake rocks. First, the intruding magmas were probably iron-enriched with a high PGE-chrome content, e.g., top of U3 Unit. These magmas subsequently intruded and assimilated BIF, which increased the iron content of the magmas and may have helped to localize the PGE-Cr mineralization. It is not clear whether or not the Cr-rich sills made a significant contribution to the PGE-Cr mineralization due, in part, to the difficulty in recognizing the effects that a partially melted or an assimilated Cr-rich sill would have on the composition of the magma. Reconcentration of the PGEs was then assisted by hydrothermal activity along structural zones, similar to those defined by Severson (1994; Fig. 14) in the Birch Lake area. The aeromagnetic map for the area shows a disruption of the magnetic contours in the vicinity of the Birch Lake prospect. This disruption may have occurred as a result of hydrothermal activity along a fault zone that destroyed or reduced the magnetic signature in the area.

REFERENCES

Alapieti, T.T., 1991, Preliminary report on the microscopic study of drill hole Du-15: Minnesota Department of Natural Resources, Division of Minerals, Report 291, 56 p.

Andrews, M.S., 1987, Contact metamorphism of the Virginia Formation at Dunka Road, Minnesota: Chemical modifications and implications for ore genesis in the Duluth Complex [M.S. thesis]: Indiana University, Bloomington, 93 p.

Andrews, M.S., and Ripley, E.M., 1989, Mass transfer and sulfur fixation in the contact aureole of the Duluth Complex, Dunka Road Cu-Ni Deposit, Minnesota: Canadian Mineralogist, v. 27, p. 293-310.

Barnes, S-J., Couture, J-F., Sawyer, E.W., and Bouchaid, C., 1993, Nickel-copper occurrences in the Belleterre-Angliers Belt of the Pontiac Subprovince and the use of Cu-Pd ratios in interpreting platinum-group element distributions: Economic Geology, v. 88, p. 1402-1418.

Bell, K., and Blenkinsop, J., 1987, Archean depleted mantle: Evidence from Nd and Sr initial isotopic ratios of carbonatites: Geochimica et Cosmochimica Acta, v. 51, p. 291-298.

Brannon, J.C., 1984, Geochemistry of successive lava flows of the Keweenawan North Shore Volcanic Group [Ph.D. Dissertation]: Washington University, St. Louis, Missouri, 312 p.

Cogulu, E.H., 1993a, Mineralogy and chemical variations of sulphides from the Crystal Lake Intrusion, Thunder Bay, Ontario: Geological Survey of Canada, Open-File 2749, 51 p.

Cogulu, E.H., 1993b, Factors controlling postcumulus compositional changes of chrome-spinels in the Crystal Lake Intrusion, Thunder Bay, Ontario: Geological Survey of Canada, Open File 2748, 79 p.

DePaolo, D.J., and Wasserburg, G.J., 1979, Petrogenetic mixing models and Nd-Sr isotopic patterns: Geochimica et Cosmochimica Acta, v. 43, p. 615-627.

Dosso, L., 1984, The nature of the subcontinental mantle: Isotopic study (strontium, lead, neodymium) of the Keweenawan volcanism of the north shore of Lake Superior [Ph.D. Dissertation]: University of Minnesota, Minneapolis, MN, 221 p.

Eckstrand, O.R., Cogulu, E.H., and Scoates, R.F.J., 1989, Magmatic Ni-Cu-PGE mineralization in the Crystal Lake layered intrusion, Ontario and the Fox River sill, Manitoba [abs.]: Minnesota Geological Survey, Information Circular 30, p. 45-46.

Geul, J.J.C., 1970, Geology of the Devon and Pardee Townships and the Stuart location: Ontario Department of Mines and Geology, Report 87, 52 p.

Green, J.C., 1986, Lithogeochemistry of Keweenawan igneous rocks; Minn. Dept. Nat. Res., Div. Minerals, Project 241-4, Open file Report, 94 p.

Grout, F.F., and Broderick, T.M., 1919, The magnetite deposits of the eastern Mesabi Range, Minnesota; Minnesota Geological Survey, Bulletin 17, 58 p.

Gundersen, J.N., and Schwartz, G.M., 1962, The geology of the metamorphosed Biwabik Iron-Formation, eastern Mesabi district, Minnesota: Minnesota Geological Survey, Bulletin 43, 139 p.

Hauck, S.A., 1993, Geology and mineralization of the Bathtub Cu-Ni area, Minnamax Cu-Ni deposit: Natural Resources Research Institute, University of Minnesota, Duluth, Unpublished Draft Report, NRRI/TR-93/48, 59 p.

Heaman, L.M., and Machado, N., 1992, Timing of Midcontinent Rift alkaline magmatism, North America: Evidence from the Coldwell Complex: Contributions to Mineralogy and Petrology, v. 110, p. 289-303.

Hulbert, L.J., and Von Gruenewaldt, G., 1985, Textural and compositional features of chromite in the Lower and Critical Zones of the Bushveld Complex south of Potgietersrus: Economic Geology, v. 80, p. 872-895.

Jensen, L.S., 1976, A new cation plot for classifying subalkaline volcanic rocks: Ontario Geological survey, Miscellaneous Paper 66, 22 p.

Jones, N.W., 1984, Petrology of the some Logan diabase sills, Cook County, Minnesota: Minnesota Geological Survey, Report of Investigations 29, 40 p.

Kuhns, M.J.P., Hauck, S.A., and Barnes, R.J., 1990, Origin and occurrence of platinum group elements, gold and silver in the South Filson Creek copper-nickel mineral deposit, Lake County, Minnesota: Natural Resources Research Institute, University of Minnesota, Duluth, Technical Report, NRRI/TR-89-15, 67 p.

Morrison, D.A., Ashwal, L.D., Phinney, W.C., Shih, C.Y., and Wooden, J.L., 1983, Pre-Keweenawan anorthosite inclusions in the Keweenawan Beaver Bay and Duluth Complexes, northeastern Minnesota: Geological Society of America Bulletin, v. 94, p. 206-221.

Mudrey, Jr., M.G., 1973, Structure and petrology of the sill on Pigeon Point, Minnesota [Ph.D. dissertation]: University of Minnesota, Minneapolis, 310 p.

Muhich, T.G., 1993, Movement of titanium across the Duluth Complex - Biwabik Iron Formation contact at Dunka Pit, Mesabi Iron Range, northeastern Minnesota [M.S. thesis]: University of Minnesota, Duluth, MN, 154 p.

Nicholson, S.W., and Shirey, S.B., 1990, Midcontinent Rift volcanism in the Lake Superior region: Sr, Nd, and Pb isotopic evidence for a mantle plume origin: Journal of Geophysical Research, v. 95, p. 10,851-10,868.

Paces, J.B., and Bell, K., 1989, Non-depleted sub-continental mantle beneath the Superior Province of the Canadian Shield: Nd-Sr isotopic and trace element evidence from Midcontinent Rift basalts: Geochimica et Cosmochimica Acta, v. 53, p. 2023-2035.

Ripley, E.M., and Al-Jassar, T.J., 1987, Sulfur and oxygen isotope studies of melt-country rock interaction, Babbitt Cu-Ni deposit, Duluth Complex, Minnesota: Economic Geology, v. 82, p. 87-107.

Ripley, E.M., and Taib, N.I., 1989, Carbon isotopic studies of metasedimentary and igneous rocks at the Babbitt Cu-Ni deposit, Duluth Complex, Minnesota: Isotope Geoscience, v. 73, p. 319-342.

Ripley, E.M., Butler, B.K., and Taib, N.I., 1992, Effects of devolatilization on the hydrogen isotopic composition of pelitic rocks in the contact aureole of the Duluth Complex, northeastern Minnesota, U.S.A.: Chemical Geology, v. 102, p. 185-197.

Ripley, E.M., Butler, B.K., Taib, N.I., and Lee, I., 1993, Hydrothermal alteration in the Babbitt Cu-Ni deposit, Duluth complex: Mineralogy and hydrogen isotope systematics: Economic Geology, v. 88, p. 679-696.

Sabelin, T., 1985, Platinum group element minerals in the Duluth Complex [abs.]: 31st Annual Institute of Lake Superior Geology, Kenora, Ontario, v. 31, p. 83- 84.

Sabelin, T., 1987, Association of platinum deposits with chromium occurrences: An overview with implications for the Duluth Complex: Skillings Mining Review, v. 76, no. 47, p. 4-7.

Sabelin, T., and Iwasaki, I., 1985, Metallurgical evaluation of chromium-bearing drill core samples from the Duluth Complex: University of Minnesota Minerals Resources Research Center, Contract Report to the Minnesota Department of Natural Resource, Division of Minerals, 58 p.

Sabelin, T., and Iwasaki, I., 1986, Evaluation of platinum group metal occurrence in Duval 15 drill core from the Duluth Complex: Internal Report, Minerals Resources Research Center, University of Minnesota, Minneapolis, 23 p.

Sabelin, T., Iwasaki, I., and Reid, K.J., 1986, Platinum group minerals in the Duluth Complex and their beneficiation behaviors: Skillings Mining Review, v. 75, no. 34, p. 4-7.

Seifert, K.E., Peterman, Z.E., and Thieben, S.E., 1992, Possible crustal contamination of Midcontinent Rift igneous rocks: Examples from the Mineral Lake intrusions, Wisconsin: Canadian Journal of Earth Sciences, v. 29, p. 1140-1153.

Severson, M.J., 1991, Geology, mineralization, and geostatistics of the Minnamax/Babbitt Cu-Ni deposit (Local Boy area), Minnesota, Part I: Geology: Natural Resources Research Institute, University of Minnesota, Duluth, Technical Report, NRRI/TR-91/13a, 96 p.

Severson, M.J., 1994, Igneous stratigraphy of the South Kawishiwi Intrusion, Duluth Complex, northeastern Minnesota: Natural Resources Research Institute, University of Minnesota, Duluth, Technical Report, NRRI/TR-93/34, 210 p..

Severson, M.J., 1997, Igneous stratigraphy and mineralization in the basal portion of the Partridge River intrusion, Duluth Complex, Allen Quadrangle, Minnesota: Natural Resources Research Institute, University of Minnesota, Duluth, Technical Report, NRRI/TR-97/17, 96 p.

Severson, M.J. and Barnes, R.J., 1991, Geology, mineralization, and geostatistics of the Minnamax/Babbitt Cu-Ni deposit (Local Boy area), Minnesota, Part II: Mineralization and geostatistics: Natural Resources Research Institute, University of Minnesota, Duluth, Technical Report, NRRI/TR-91/13b, 221 p.

Severson, M.J., Patelke, R.L., Hauck. S.A., and Zanko, L.M., 1996, The Babbitt copper-nickel deposit Part C: Igneous geology, footwall lithologies, and cross-sections: Natural Resources Research Institute, University of Minnesota, Duluth, Technical Report, NRRI/TR-94/21c, 79 p.

Table 1. List of samples analyzed by various geochemical methods.

Sample (DDH)	Rock Type	From (ft)	To (ft)	Geo Chem	Stable Isotopes	Radiogenic Isotopes	PGEs
U3 Unit							
BL-89-2	Melatroctolite	2527.0	2532.0	X	X		X
	Melatroctolite	2538.0	2542.0	X	X		X
	Melatroctolite	2553.4	2557.0	X	X		X
	Augite Troc.	2566.0	2571.0	X	X	X	X
	Gran. Troc.	2575.0	2579.5	X	X		X
D15-W1	Melatroctolite	2319.0	2325.7	X	X	X	X
	Melatroctolite	2326.5	2331.0	X	X		X
	Massive Oxide	2339.5	2344.5	X	X		X
	Massive Oxide	2350.0	2354.8	X	X	X	X
	Massive Oxide	2355.5	2360.0	X	X		X
	Melatroctolite	2372.0	2373.0	X	X		X
	Melatroctolite	2377.0	2381.5	X	X		X
	Ox. Melatroc.	2401.0	2405.0	X	X	X	X
	Ox. Melatroc.	2411.8	2417.0	X	X		X
	Ox. Melatroc.	2420.3	2426.0	X	X	X	X
	Pyroxenite	2434.0	2437.5	X	X		X
	Ox. Melatroc.	2439.0	2441.7	X	X		X
	Pyroxenite	2446.0	2449.0	X	X	X	X
BIF							
B2-1	Submember C	261.7	265.6	X	X	X	X
	Submember M	474.0	477.0	X	X	X	X
	Submember P	578.0	580.0	X	X	X	X
B2-2	Submember F	352.0	354.0	X		X	X
	Submember L	462.5	466.0	X			X
SILL - VF							
B1-140	Cr-rich Sill/Virg Sill	1942.0	1943.0	X			X
B1-148	Cr-rich Sill/Virg Sill	1979.9	1980.8	X		X	X
B1-131	Cr-rich Sill/Virg Sill	1910.0	1910.8	X			X
B1-58	Cr-rich Sill/Virg Sill	1506.0	1507.0	X			X

Sample (DDH)	Rock Type	From (ft.)	To (ft.)	Geo Chem	Stable Isotopes	Radiogenic Isotopes	PGEs
B1-360	Cr-rich Sill/MG Unit*	1708.0	1709.0	X			X
SILL - BIF							
B1-171	Cr-rich B-Sill	637.0	638.0	X	X		X
B1-179	Logan-type C-Sill**	784.5	785.8	X	X		X
B2-5	Logan-type C-Sill	259.0	260.0	X	X	X	X
BLOCK 12	Logan-type C-Sill	Outcrop		X	X	X	X
BLOCK 20	Logan-type C-Sill	Outcrop		X	X	X	X
CRUSHER #2	Cr-rich Sill C-Sill	Outcrop		X	X	X	X
Standards	MRG-1, SARM-12			2			
Totals				27	34	15	26

NOTE: * See Severson et al., 1996
** See Severson, 1997

Table 2. PGE, Cu, Ni, Au, Ag, and Cr analyses from the Birch Lake area, South Kawishiwi Intrusion, Duluth Complex.

Sample Number	Rock Type	Cl ppm	Cu ppm	Ni ppm	S Wt. %	Ag ppm	Pt ppb	Pd ppb	Au ppb	Ir ppb	Os ppm	Rh ppm	Ru ppm	Re ppm	Cr ppm
Logan-type Sills (C-Sills)															
BLOCK 12		790	336	67	0.041	0.5	6.83	12.51	1.01	0.03	<0.89	0.55	<5.80	0.22	43
BLOCK 20		583	253	46	0.053	0.6	6.27	8.90	2.48	0.08	<0.98	<0.49	<5.00	0.30	26
Cr-Rich Sills															
CRUSHER #2/C-Sill		1330	13.5	369	0.026	0.1	14.39	9.10	7.71	0.70	<1.40	0.76	<7.20	0.42	860
B1-131-1909.0/Virg Sill		186	314	291	0.220	<0.5	4.21	6.40	1.83	0.44	<0.93	0.42	<4.80	0.35	800
B-140-1942.0/Virg Sill		99	115	232	0.130	<0.5	6.03	8.87	2.84	0.76	0.90	0.44	<2.10	0.43	800
B1-148-1979.0/Virg Sill		1310	99	806	0.050	<0.5	6.36	9.45	3.58	1.08	2.40	0.79	2.10	0.25	2327
Biwabik Iron-Formation															
B2-1-261.7	Smbr C	1150	10.2	1	0.215	0.4	2.45	3.42	0.51	0.07	<0.55	0.44	<3.70	0.06	24
B2-1-474.0	Smbr M	184	4.5	<1	0.010	0.5	<4.60	<4.20	0.30	0.03	<1.00	<0.39	<6.80	<0.40	20
B2-1-578.0	Smbr P	158	16.0	<1	0.033	1.4	2.12	<2.50	0.33	0.02	<0.48	<0.15	<3.90	<0.07	18
B2-2-352.0	Smbr F	147	9.6	3	0.017	0.4	<2.40	<0.82	0.29	0.03	0.48	<0.07	<2.00	<0.07	30
B2-2-462.5	Smbr L	122	4.2	<1	0.014	0.8	<2.60	<1.20	0.13	<0.01	<0.50	<0.14	<4.40	<0.09	17
BL-89-2															
BL-89-2-2527.0	MT	3260	8090	3320	0.898	2.8	571.30	1272.15	88.76	25.86	17.38	63.76	78.06	0.88	1100
BL-89-2-2538.0	MT	1550	7010	3100	0.856	1.9	679.92	1130.04	143.30	25.71	14.47	45.54	69.00	<0.70	2000
BL-89-2-2553.8	MT	847	3640	1580	0.435	1.4	313.08	539.30	71.77	15.13	9.17	35.44	46.08	<0.61	2300
BL-89-2-2566.0	AGT	363	381	378	0.056	0.3	15.48	19.12	1.31	0.17	<1.40	<0.45	<10.00	<0.18	180
BL-89-2-2575.0	T	253	3450	1020	0.392	0.9	177.07	386.91	0.02	8.99	7.59	19.84	29.78	0.58	230
D15-W1															

Sample Number	Rock Type	Cl ppm	Cu ppm	Ni ppm	S Wt. %	Ag ppm	Pt ppb	Pd ppb	Au ppb	Ir ppb	Os ppm	Rh ppm	Ru ppm	Re ppm	Cr ppm
D15-W1-2326.5	MT	528	3920	1000	0.383	1.8	769.34	1119.90	125.24	22.98	20.90	42.31	75.75	<0.97	1800
D15-W1-2339.5	Mas Ox	4720	2710	1590	0.340	0.6	270.37	231.30	35.33	6.26	3.66	9.62	6.50	?	790
D15-W1-2355.5	Mas Ox	7840	1600	1240	0.196	1.0	63.46	153.97	10.93	1.79	<2.2	5.37	<14.00	<0.27	69
D15-W1-2377.0	MT	2730	1930	1860	0.388	0.8	69.53	136.02	8.82	3.68	2.63	8.38	16.18	0.29	390
D15-W1-2401.0	Ox MT	1450	4450	1960	0.531	1.7	924.13	1014.65	80.78	46.04	29.26	75.00	112.40	<0.60	7200
D15-W1-2411.8	Ox MT	1710	4850	2060	0.690	1.5	384.14	475.76	41.00	15.32	9.13	27.13	32.00	<0.37	2600
D15-w1-2420.3	Ox MT	846	1980	1390	0.343	0.7	216.33	265.85	15.83	10.23	6.38	21.25	30.33	<0.42	4100
D15-W1-2434.0	Pyrox.	155	2100	713	0.452	0.8	136.45	210.43	18.94	5.55	4.33	12.32	11.46	0.84	510
D15-W1-2439.0	Ox MT	1010	747	2000	0.503	0.2	37.09	66.32	10.97	3.76	2.58	5.56	18.42	<0.32	1500
D15-W1-2446.0	Pyrox.	147	730	465	0.407	0.3	18.73	30.51	2.33	1.56	<2.5	3.72	<13.00	0.74	350

Table 3. Stable isotope data, Birch Lake area, South Kawishiwi Intrusion, Duluth Complex.

Sample No.	Rock Type	$\delta^{18}O$	δ^{13} LTC	δ^{13} HTC	δD	$\delta^{34}S$
DDH No. & Footage		‰ SMOW	‰ PDB	‰ PDB	‰ SNOW	‰ CDT
D15-W1-2325.0-2325.7	Melatroc.	3.9	-10.2	-18.0	-92	2.7
D15-W1-2327.3-2327.8	Melatroc.	3.9	-14.7	-17.1	-98	1.8
D15-W1-2340.9-2341.5	Mass. Oxide	3.3	-11.3	-19.2	-82	3.2
D15-W1-2354.2-2354.8	Mass. Oxide	2.5	-10.5	-16.0	-87	4.5
D15-W1-2359.6-2360.0	Mass. Oxide	3.3	-12.4	-17.7	-90	6.5
D15-W1-2372.0-2372.7	Melatroc.	3.3	-6.5	-18.6	-82	7.0
D15-W1-2378.8-2379.3	Melatroc.	1.8	-10.6	-14.9	-84	5.5
D15-W1-2402.5-2402.9	Ox Melatroc.	4.9	-16.5	-16.6	-87	3.0
D15-W1-2415.2-2415.8	Ox Melatroc.	6.5	-19.7	-15.4	-89	5.7
D15-W1-2423.0-2423.5	Ox Melatroc.	5.4	-9.2	-15.9	-86	6.0
D15-W1-2435.3-2435.8	Pyroxenite	6.2	-5.1	-15.6	-74	6.3
D15-W1-2439.8-2440.3	Ox Melatroc.	3.3	-9.5	-16.6	-76	7.4
D15-W1-2447.6-2448.2	Pyroxenite	6.8	-6.0	-14.4	-68	9.6
BL-89-2-2531.1-2531.7	Melatroc.	3.9	-10.5	-21.6	-86	2.6
BL-89-2-2541.0-2541.6	Melatroc.	3.9	-8.5	-14.7	-86	2.9
BL-89-2-2555.8-2556.3	Melatroc.	4.9	-13.7	-17.7	-87	2.0
BL-89-2-2566.3-2566.8	Augite Troc.	6.3	-14.8	-20.2	-75	2.3
BL-89-2-2576.4-2577.1	Troc.- gran.	4.4	-10.1	-15.8	-77	3.6
B2-1-264.7-265.2	BIF - Smbr C	10.5	-21.4	-26.7	-113	no S
B2-1-474.4-475.0	BIF - Sbmr M	16.5	-15.8	-20.4	-86	no S
B2-1-578.0-578.6	BIF - Sbmr P	16.7	-18.0	-19.7	-84	11.0
B1-171-637.0-638.0	Cr-rich Sill/B-Sill	10.3	-12.9	-19.7	-77	11.2
Crusher #2 Outcrop-PMM	Cr-rich Sill/C-Sill	14.4	-16.9	-21.1	-67	10.8
B1-179-784.5-785.8	Logan Sill/C-Sill	9.4	-14.1	-20.4	-88	5.6

Sample No.	Rock Type	$\delta^{18}O$	δ^{13} LTC	δ^{13} HTC	δD	$\delta^{34}S$
DDH No. & Footage		‰ SMOW	‰ PDB	‰ PDB	‰ SNOW	‰ CDT
B2-5-259.0-260.0	Logan Sill/C-Sill	8.8	-15.8	-21.8	-93	11.1
Block 12 Outcrop-PMM	Logan Sill/C-Sill	9.2	-14.3	-18.1	-80	9.9
Block 20 Outcrop-PMM	Logan Sill/C-Sill	10.1	-12.2	-21.7	-93	6.7

Table 4a. Sm-Nd analyses from the Birch Lake area, South Kawishiwi Intrusion, Duluth Complex.

Sample No.	Rock Type	Sm ppm	Nd ppm	147Sm/ 144Nd	143Nd/ 144Nd	εNd	T(DM)	εNd (1100)
D15-W1-2319-2324	Melatroc.	0.86	3.93	0.13602	0.512178	-8.97	1691	-0.42
D15-W1-2350-2354	Mass. Oxide	0.36	1.67	0.13507	0.512161	-9.31	1705	-0.63
D15-W1-2401-2405	Ox Melatroc.	0.94	4.19	0.13831	0.512007	-12.30	2094	-4.09
D15-W1-2420.3-2426	Ox Melatroc.	0.69	3.32	0.12922	0.511774	-16.85	2295	-7.37
D15-W1-2446-2449	Pyroxenite	8.03	36.49	0.13621	0.511535	-21.52	3010	-13.04
BL-89-2-2566-2571	Augite Troc.	3.42	15.69	0.13492	0.512133	-9.84	1755	-1.14
B2-1-261.7-265.6	BIF - Smbr C	1.38	7.42	0.11500	0.511475	-22.69	2431	-11.21
B2-1-474-477	BIF - Smbr M	0.58	3.21	0.11233	0.511650	-19.28	2096	-7.42
B2-1-578-580	BIF - Smbr P	0.26	1.18	0.13514	0.511722	-17.87	2580	-9.23
B2-2-352-354	BIF - Smbr F	0.56	2.95	0.12011	0.511691		2207	1.2
B1-148-1979-1983	Cr-rich Sill/Virg Sill	2.136	8.893	0.14864	0.512170	-9.12	2042	-2.36
Crusher #2 - PMM	Cr-rich Sill/C-Sill	3.072	13.161	0.14443	0.512136	-9.80	1993	-2.44
B2-5-260-265	Logan Sill/C-Sill	8.847	38.169	0.14342	0.512239	-7.78	1737	-0.27
Block 12 - PMM	Logan Sill/C-Sill	10.199	46.735	0.13503	0.512135	-9.82	1755	-1.14
Block 20 - PMM	Logan Sill/C-Sill	8.518	39.499	0.13344	0.512119	-10.12	1749	-1.21

Note: Analyses and calculations done under contract by Dr. Stephen Goldberg, Geology Department, University of North Carolina at Chapel Hill.

Table 4b. Rb-Sr analyses from the Birch Lake area, South Kawishiwi Intrusion, Duluth Complex.

Sample No	Rock Type	87Rb/8	87Sr/86Sr	Rb ppm	Sr ppm	87Sr/86Sr (T)	εSr (1100 Ma)
D15-W1-2319-2324	Melatroc.	0.0845	0.706285	4.38	149.97	0.704955	27.12
D15-W1-2350-2354	Mass. Oxide	0.1045	0.706671	1.66	45.84	0.705026	28.13
D15-W1-2401-2405	Ox Melatroc.	0.0893	0.708590	4.16	134.95	0.707184	58.83
D15-W1-2420.3-2426	Ox Melatroc.	0.0848	0.708414	3.92	133.88	0.707079	57.34
D15-W1-2446-2449	Pyroxenite	0.1301	0.710484	24.13	536.74	0.708436	76.64
BL-89-2-2566-2571	Augite Troc.	0.1538	0.707012	17.15	322.53	0.704591	21.94
B2-1-261.7-265.6	BIF - Smbr C	0.0966	0.710080	1.44	43.23	0.707297	60.44
B2-1-474-477	BIF - Smbr M	0.0875	0.709807	0.84	27.78	0.707286	60.29
B2-1-578-580	BIF - Smbr P	0.0571	0.710433	0.23	11.81	0.708788	81.65
B2-2-352-354	BIF - Smbr F	0.0856	0.710836	0.72	24.18	0.708370	75.70
B1-148-1979-1983	Cr-rich Sill/Virg Sill	0.0443	0.705841	2.06	133.91	0.705143	29.80
Crusher #2 - PMM	Cr-rich Sill/C-Sill	0.4975	0.714335	40.19	232.74	0.706504	49.15
B2-5-260-265	Logan Sill	0.0293	0.706806	5.24	517.86	0.706345	46.89
Block 12 - PMM	Logan Sill	0.3626	0.712181	57.52	459.26	0.706473	48.71
Block 20 - PMM	Logan Sill	0.3197	0.712150	64.96	588.05	0.707117	57.88

Note: Analyses and calculations done under contract by Dr. Stephen Goldberg, Geology Department, University of North Carolina at Chapel Hill.

Table 4c. U-Pb analyses from the Birch Lake area, South Kawishiwi Intrusion, Duluth Complex.

Sample No.	Rock Type	206Pb/ 204Pb	207Pb/ 204Pb	208Pb/ 204Pb	U ppm	Pb ppm	238U/ 204Pb	235U/ 204Pb	206Pb/ 204PB (T)	207Pb/ 204PB (T)
D15-W1-2319-2324	Melatroc.	17.932	15.480	37.529	0.152	2.432	3.8901	0.0282	17.208	15.425
D15-W1-2350-2354	Massive Oxide	17.472	15.484	37.175	0.065	2.837	1.4082	0.0102	17.210	15.464
D15-W1-2401-2405	Oxide Melatroc.	16.903	15.361	36.545	1.159	5.427	1.2885	0.0093	16.663	15.342
D15-W1-2420.3-2426	Oxide Melatroc.	17.173	15.414	36.843	0.112	2.738	2.4933	0.0181	16.709	15.378
D15-W1-2446-2449	Pyroxenite	16.853	15.288	36.782	0.350	7.105	2.9794	0.0216	16.298	15.245
BL-89-2-2566-2571	Augite Troctolite	19.289	15.574	38.834	0.109	2.661	2.6026	0.0189	18.805	15.537
B2-1-261.7-265.6	BIF - Smbr C	21.685	15.915	38.834	0.023	0.750	2.0290	0.0147	20.947	15.824
B2-1-474-477	BIF - Smbr M	18.287	15.576	37.949	0.039	0.709	3.4831	0.0253	17.020	15.420
B2-1-578-580	BIF - Smbr P	16.900	15.276	36.617	0.019	0.470	2.4516	0.0178	16.008	15.167
B2-2-352-354	BIF - Smbr F	18.145	15.538	39.552	0.033	0.519	4.1256	0.0299	16.644	15.354
B1-148-1979-1983	Cr-rich Sill/Virg Sill	18.075	15.607	37.096	0.088	2.033	2.6752	0.0194	17.577	15.569
Crusher #2 - PMM	Cr-rich Sill/C-Sill	17.930	15.584	36.977	0.451	16.507	1.6872	0.0122	17.616	15.560
B2-5-260-265	Logan Sill/C-Sill	18.688	15.658	37.243	0.466	4.054	7.0942	0.0514	17.368	15.557
Block 12 - PMM	Logan Sill/C-Sill	19.474	15.687	38.969	0.985	8.105	7.7665	0.0563	18.029	15.577
Block 20 - PMM	Logan Sill/C-Sill	18.844	15.672	37.690	1.447	11.834	7.7394	0.0561	17.404	15.563

Note: Analyses and calculations done under contract by Dr. Stephen Goldberg, Geology Department, University of North Carolina at Chapel Hill.

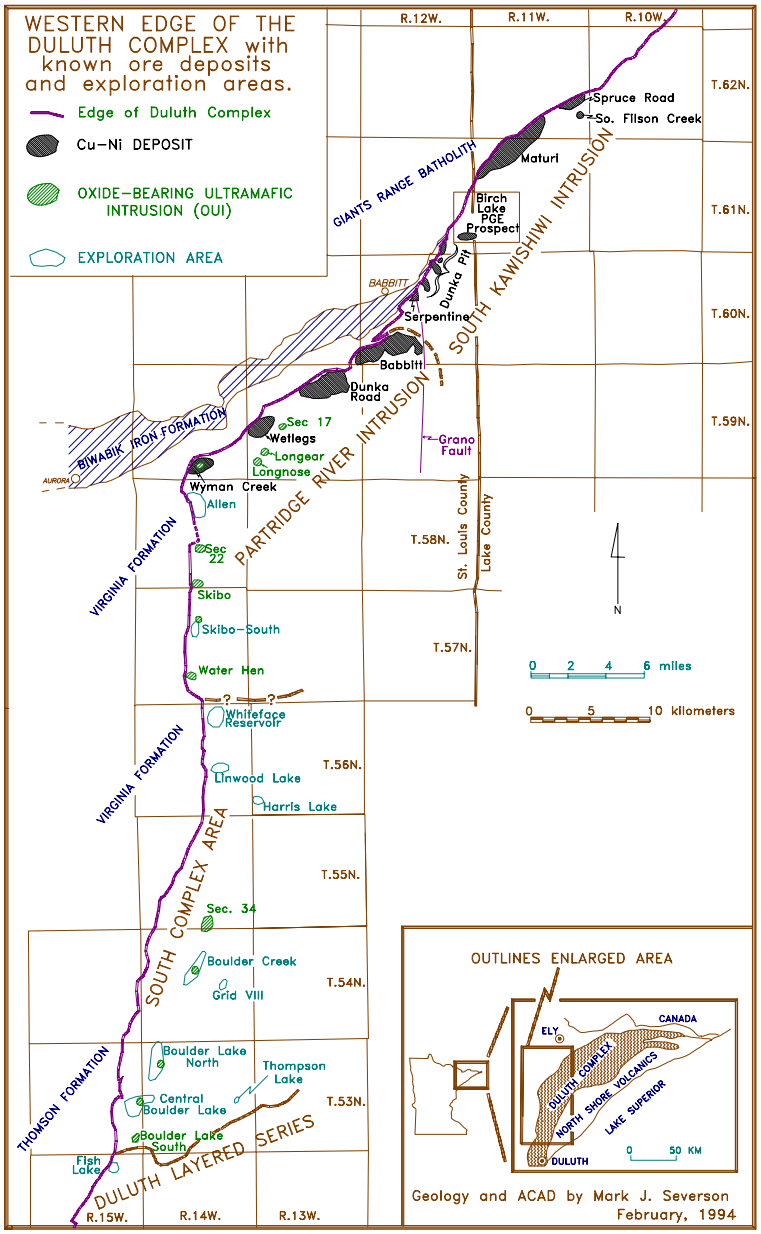

Figure 1. Location map showing Birch Lake study area along the western margin of the Duluth Complex.

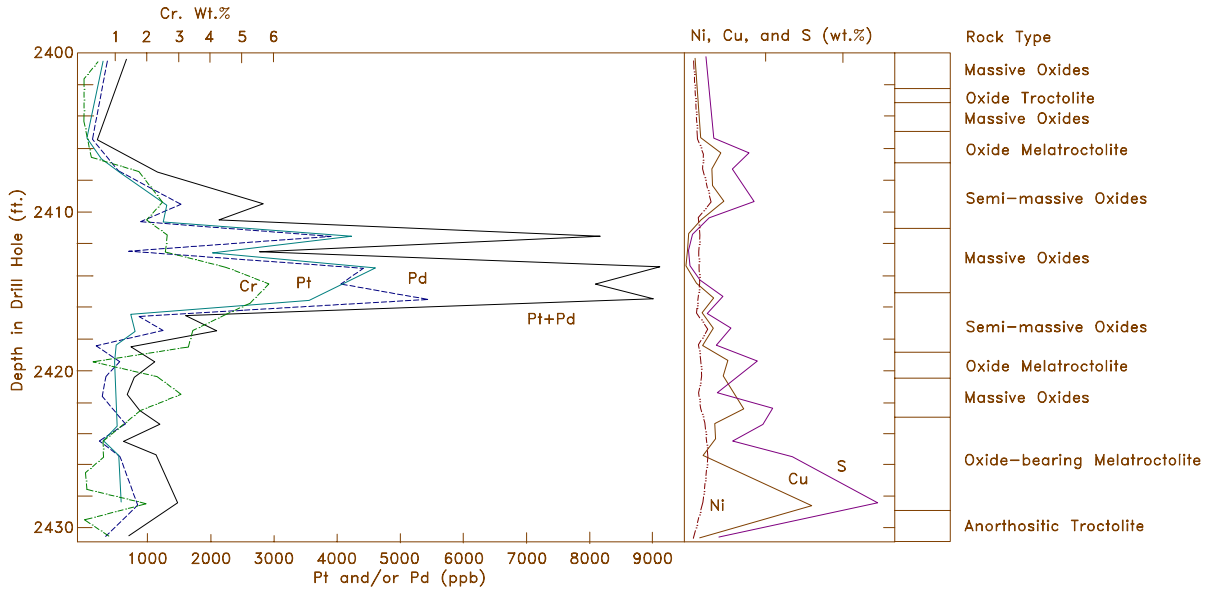

Figure 2. Diagram of PGE-Cr-Cu-Ni-S values in Du-15 from 2,400 ft. to 2,435 ft. (Data from Sabelin and Iwasaki, 1986, and geology from Severson, 1994.)

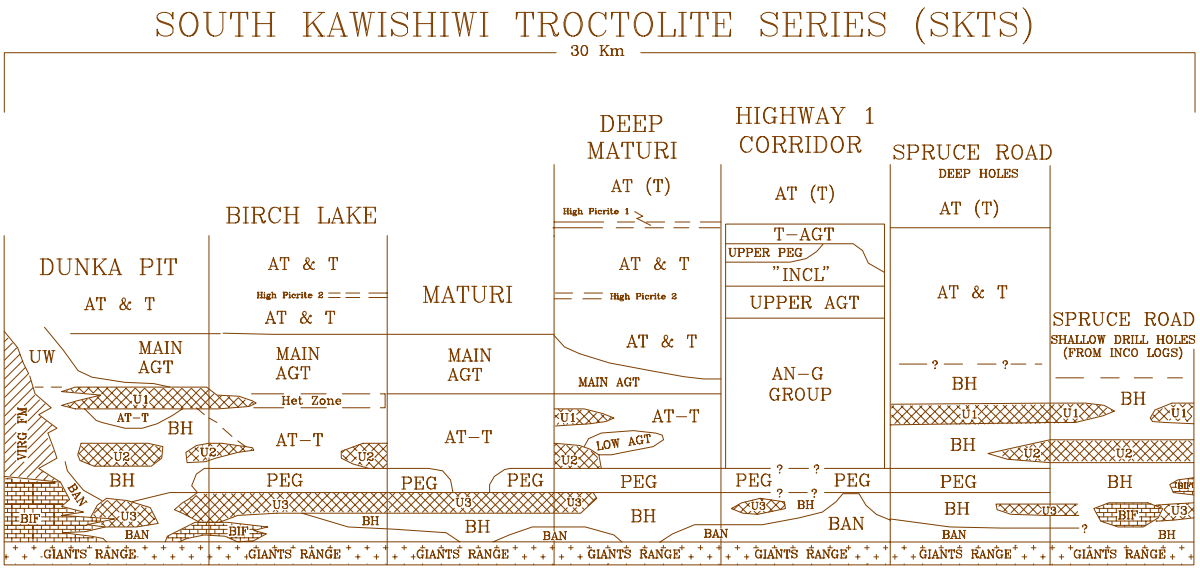

Figure 3. Schematic cross-section of the igneous stratigraphy in the South Kawishiwi Intrusion (from Severson, 1994). Stratigraphic units from bottom to top are: **BAN** - Bottom Augite Troctolite and Norite zone; Heterogeneous mixture of augite troctolite and norite (both sulfide-bearing), containing local inclusions of BIF and Giants Range Batholith (GRAN); **BH** - Basal Heterogeneous zone; The BH is the main sulfide-bearing ore zone in each of the Cu-Ni deposits; **U3** - Ultramafic 3 Unit; A package of alternating layers of ultramafic and troctolitic rocks. U3 typically contains massive oxide horizons and/or BIF inclusions and is generally sulfide-bearing; **PEG** - Pegmatitic unit of Foose (1984); A poorly defined unit in which pegmatoids and gradational pegmatite zones are sporadically present; **U2** - Ultramafic 2 Unit; A package of alternating layers of ultramafic and troctolitic rocks; massive oxide layers are only rarely present; **AT-T** - Anorthositic Troctolite to Troctolite zone; Homogeneous package of both rock types that are gradational into each other; **U1** - Ultramafic 1 Unit; Package of alternating layers of ultramafic and troctolitic rocks - massive oxides are totally lacking; **UW** - Updip Wedge; Package of heterogeneous sulfide-bearing troctolite that occurs in the western portion of the Dunka Pit area and extends southwestward to the Serpentine deposit. The UW unit only occurs where the Virginia Formation is present at the basal contact; **MAIN AGT** - Delineated by a zone where augite troctolite is the dominant rock type; **AT&T** - Thick, monotonous zone of anorthositic troctolite and troctolite with minor augite troctolite and troctolitic anorthosite. The AT&T unit also contains two ultramafic horizons tentatively called the High Picrite #1 and #2; **AT(T)** - Thick, monotonous zone of anorthositic troctolite to troctolite containing minor troctolite and rare augite troctolite zones; **Highway One Corridor Rocks** - A thick stratigraphic sequence (large raft of Anorthositic Series) delineated in 5 deep drill holes. The most definitive rock types of the sequence are the AN-G GROUP (intermixed anorthositic and gabbroic rocks) and the "Incl" unit, which is a fine-grained, granular inclusion of magnetite-rich basalt.

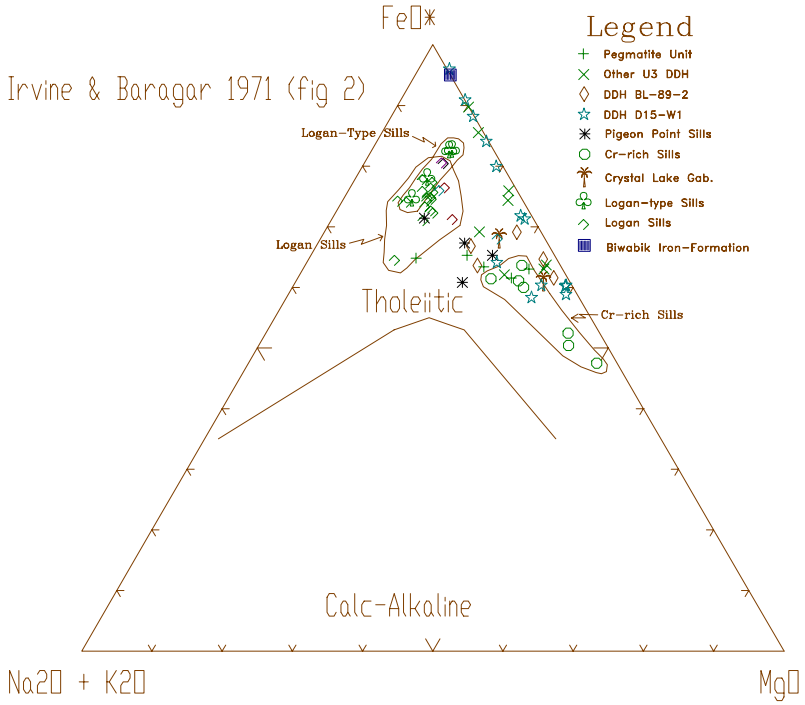

Figure 4. AFM (Jensen, 1976) diagram showing the dual differentiation trends in the troctolitic rocks and the geochemical differences between the Logan-type and Cr-rich sills. Logan sill data from Jones (1984).

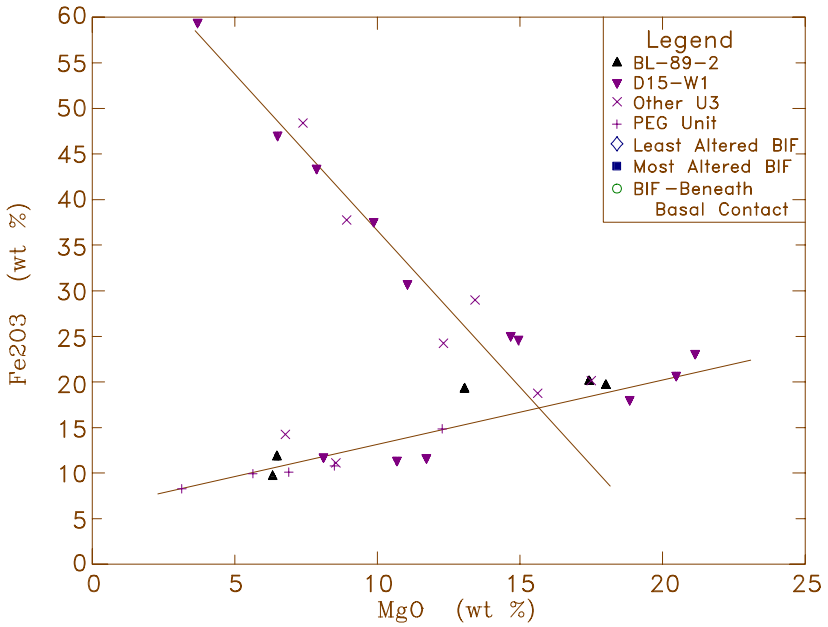

Figure 5. Fe_2O_3 vs. MgO diagram illustrating the dual differentiation trends within the troctolitic rocks of U3 Unit.

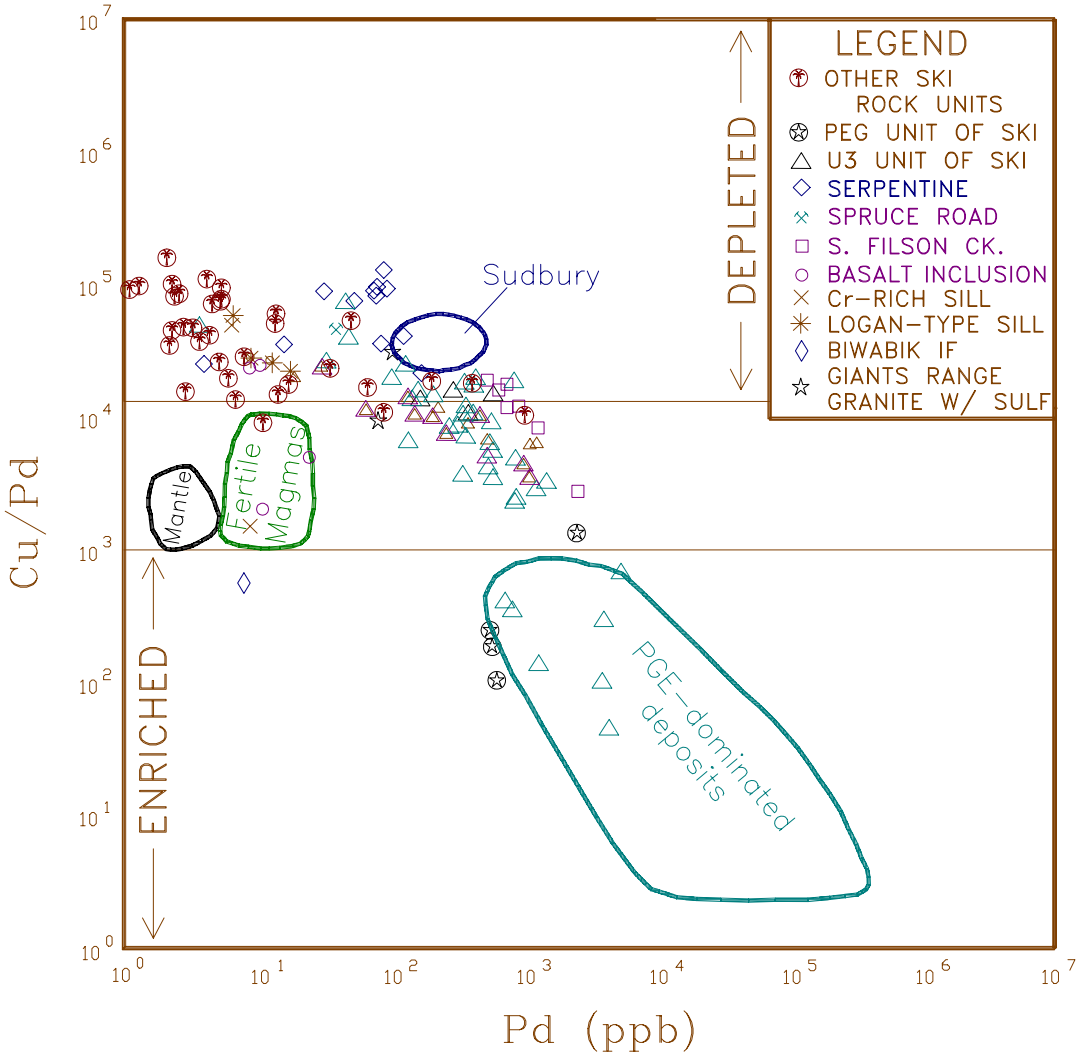

Figure 6. Cu\Pd vs. Pd diagram of Barnes et al. (1993) showing the enrichment of the U3 Unit compared to other South Kawishiwi unit samples. Data from this study, Kuhns et al. (1990) and Severson (1991, 1994).

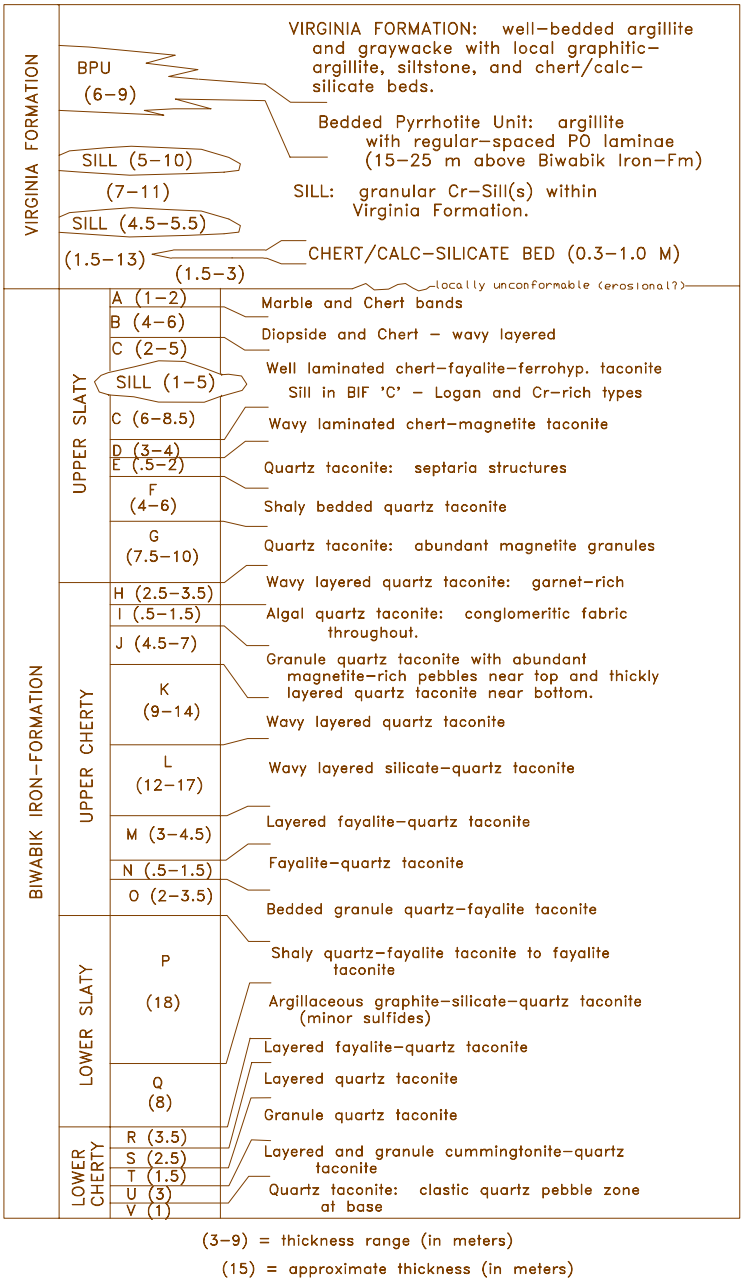

Figure 7. Generalized stratigraphic section of the Virginia Formation and underlying Biwabik Iron Formation showing approximate location of Cr-rich and Logan-type sills (after Gundersen and Schwartz, 1962, and Severson, 1994).

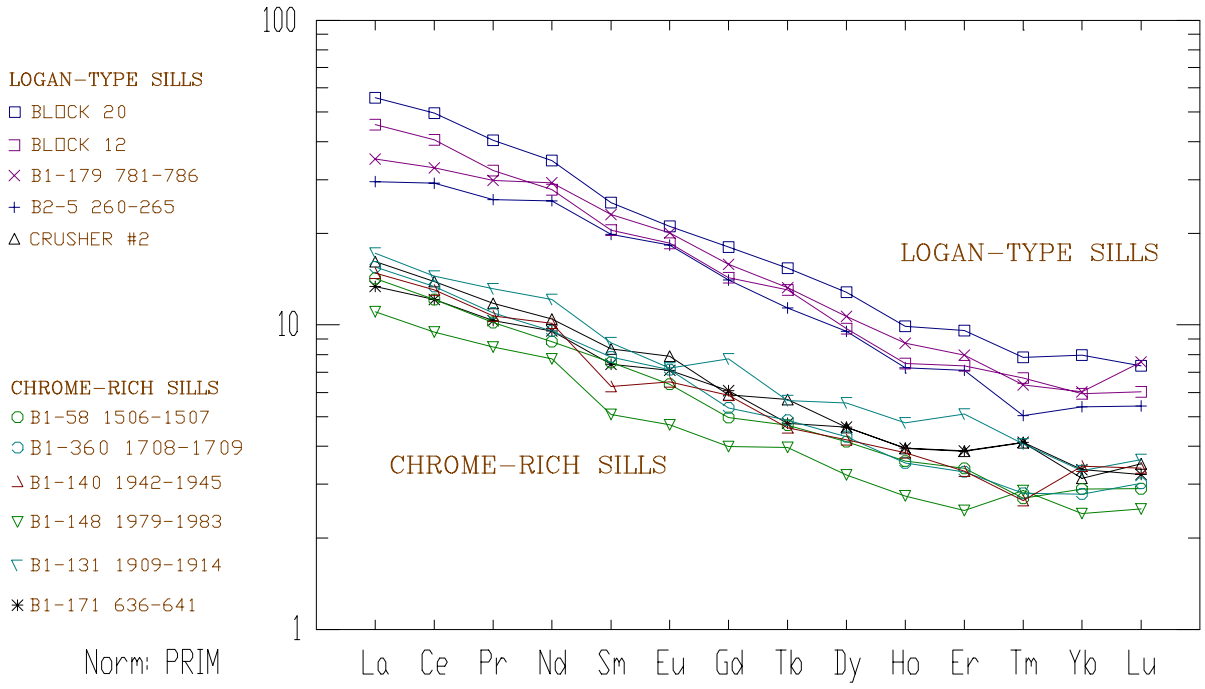

Figure 8. Normalized rare-earth element diagram illustrating the REE differences between the Logan-type and Cr-rich sills.

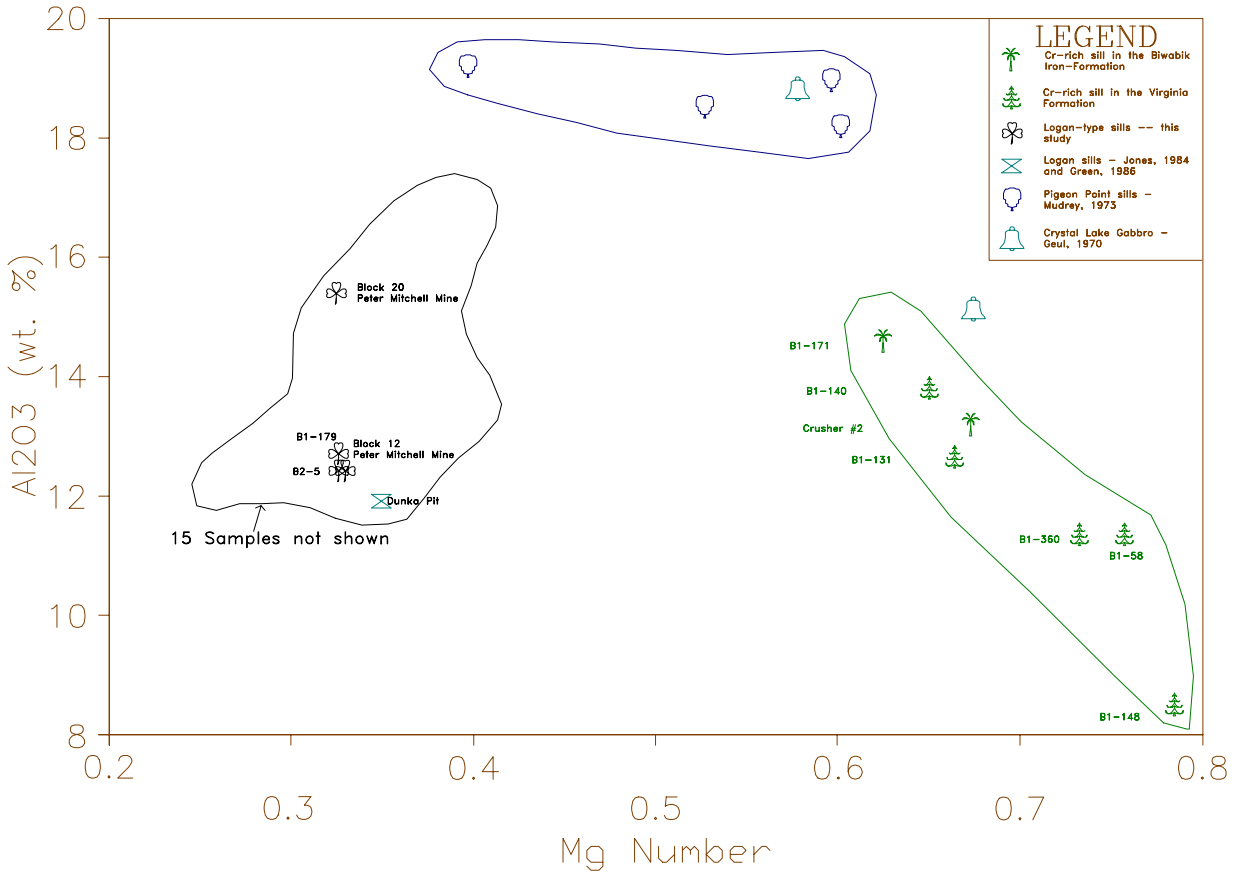

Figure 9. Mg# vs. Al_2O_3 illustrating the geochemical differences between the Logan-type, Cr-rich, and Pigeon Point sills and samples from the Crystal Lake Intrusion.

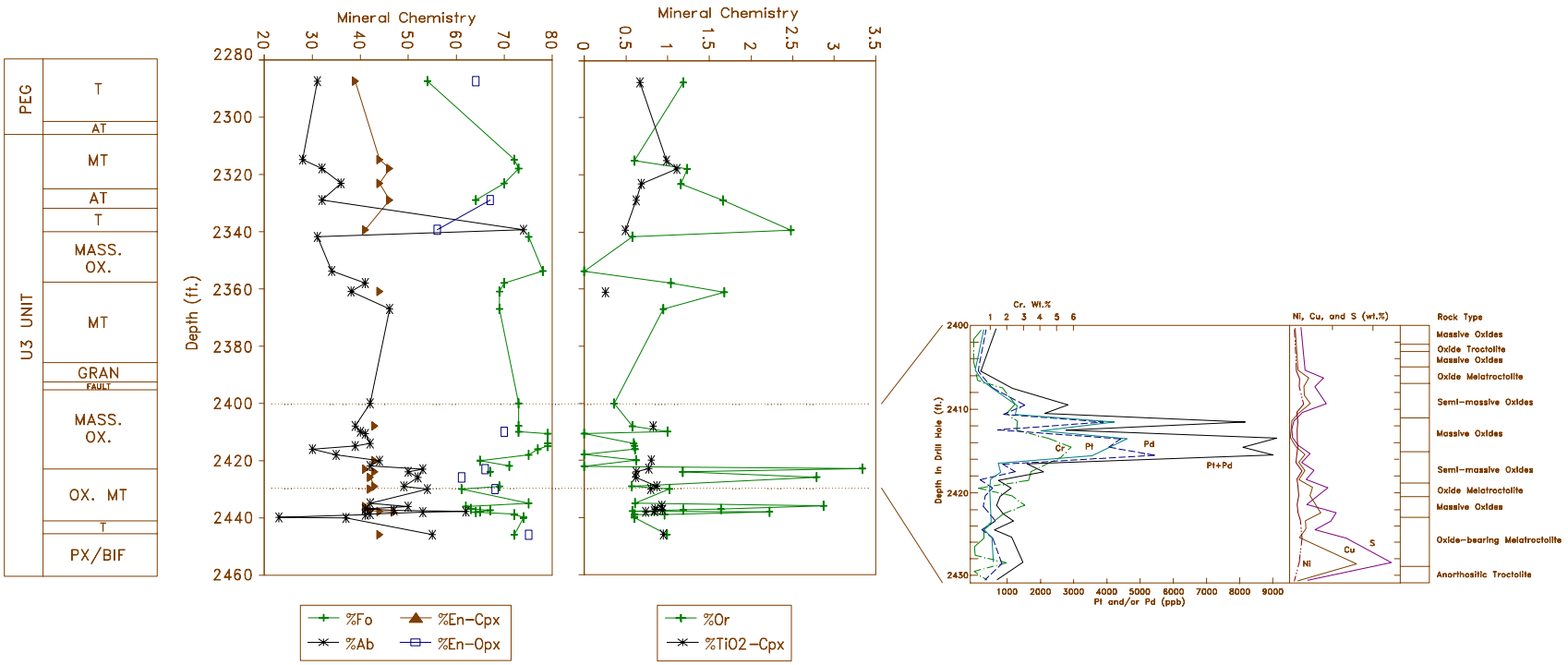

Figure 10. Du-15 downhole mineral chemistry for olivine, pyroxene, and plagioclase with geological units of Severson (1994). Note the changes in mineral chemistry at the top of the U3 Unit and for internal units within the U3 Unit. The top of the PEG Unit is not shown; only one point was collected near the base of the unit.

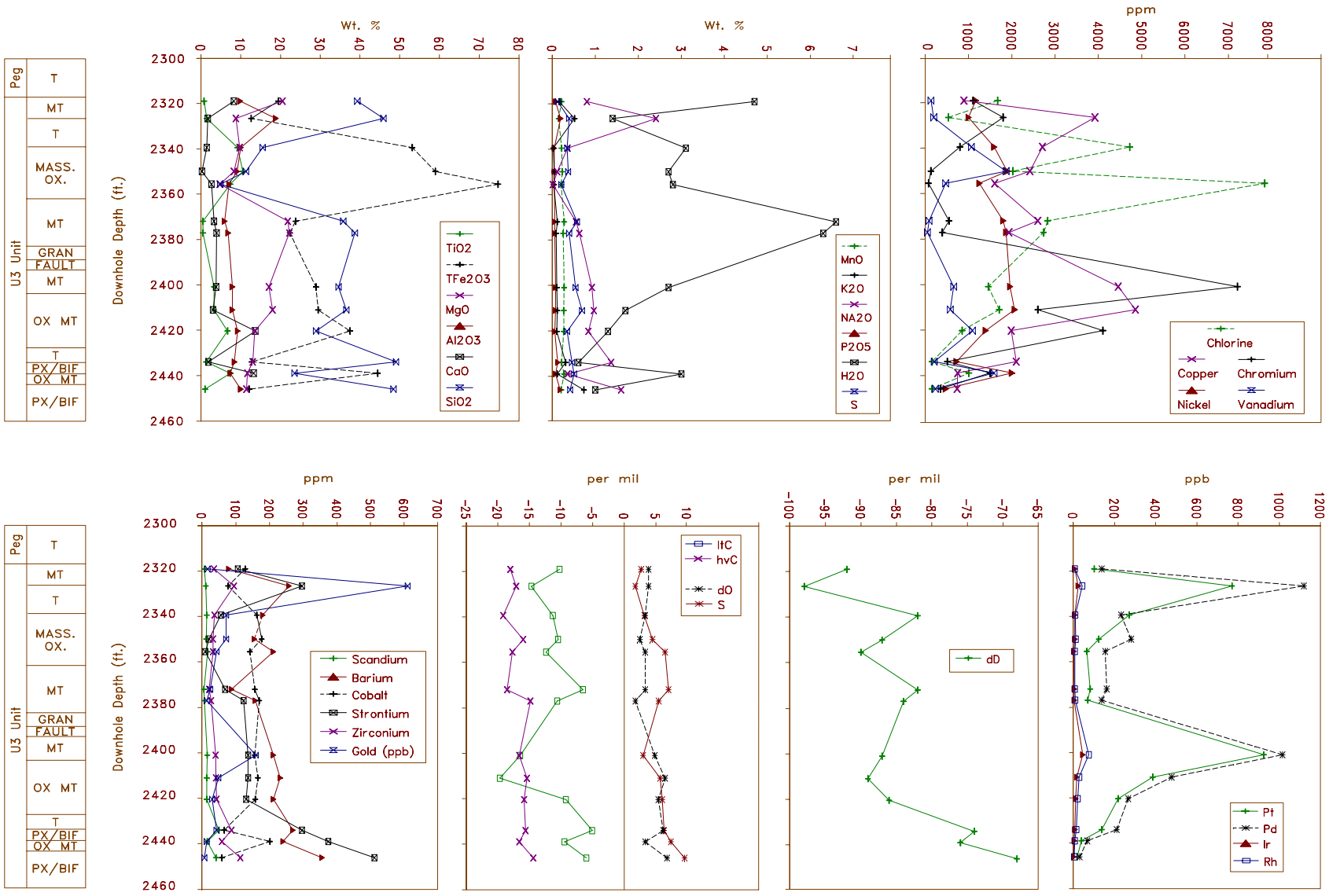

Figure 11. Downhole geochemical changes for Du-15 (top half) wedge D15-W1 (bottom half) showing changes in major and trace element and base metal chemistry using geology of Severson (1994).

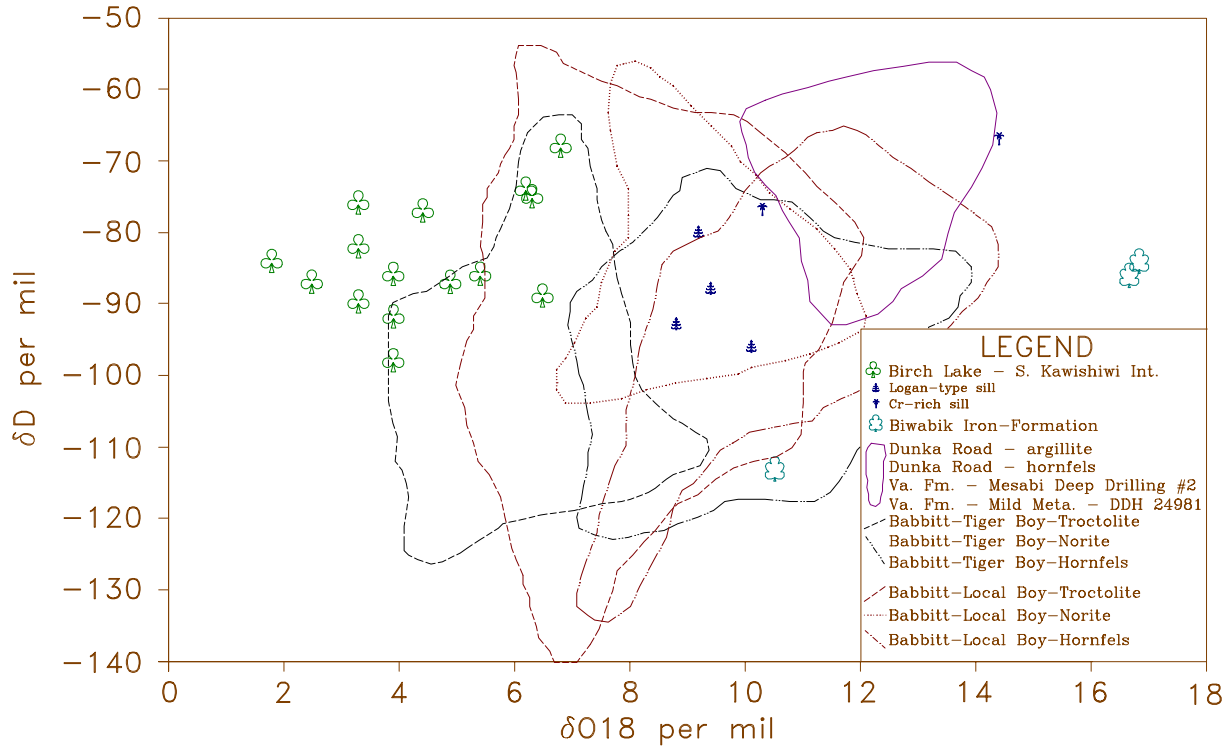

Figure 12. MD vs. M^{18}O for unmetamorphosed and metamorphosed pelitic rocks of the Virginia Formation and for igneous rocks of the Partridge River and South Kawishiwi intrusions. Birch Lake samples are shown as clover leaves.

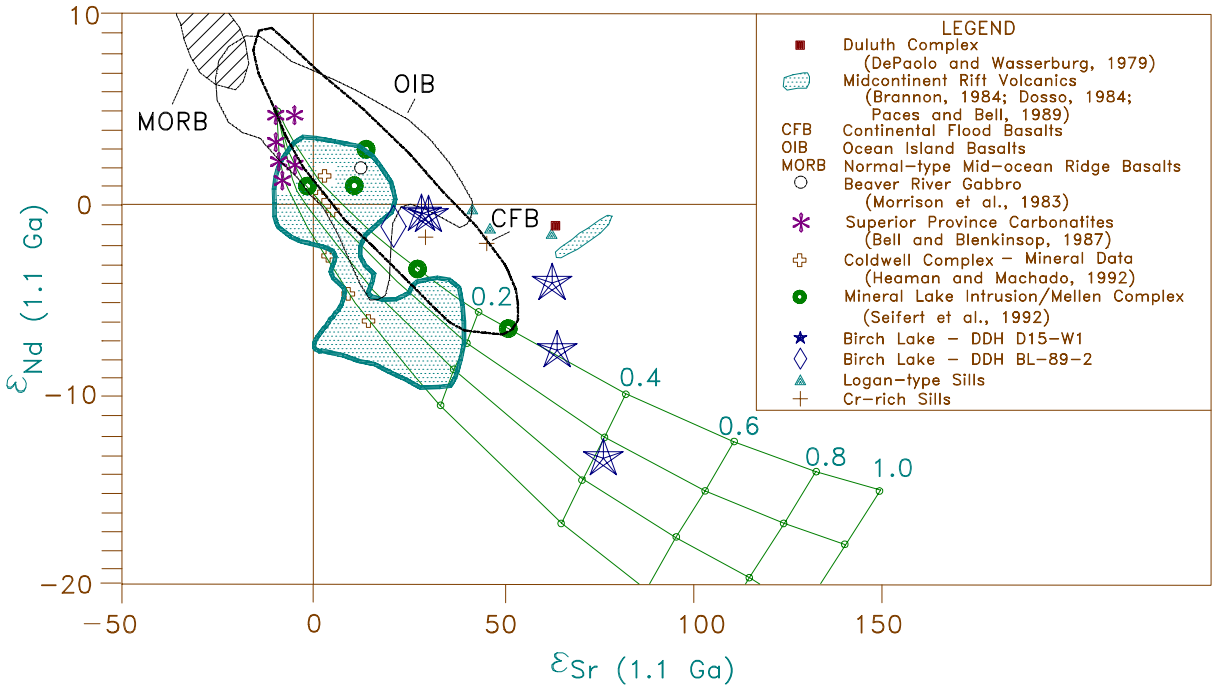

Figure 13. gNd vs. gSr at T=1,100 (after Seifert et al., 1992) for various Midcontinent Rift System intrusive and extrusive rocks. Mixing curves for four crustal components, according to the amount of crustal component, from 1.0 at high gSr values to 0 at the gNd = +5 end in 20% increments. The upper and lower curves represent crustal components with gNd and gSr values of (-15, 150), (-18, 140), (-21, 130), and (-24, 120) and are based on the older Archean rocks being more depleted than younger Archean rocks (from Seifert et al., 1992). Note the decrease in gNd and increase of gSr for samples (stars) from the Du-15 wedge D15-W1 (top to bottom and left to right), indicating increasing crustal contamination downhole. Note also the difference between the Logan-type and Cr-rich sills and that none of the samples analyzed in this study plot within the field that represents the extrusive rocks of the Midcontinent Rift System.

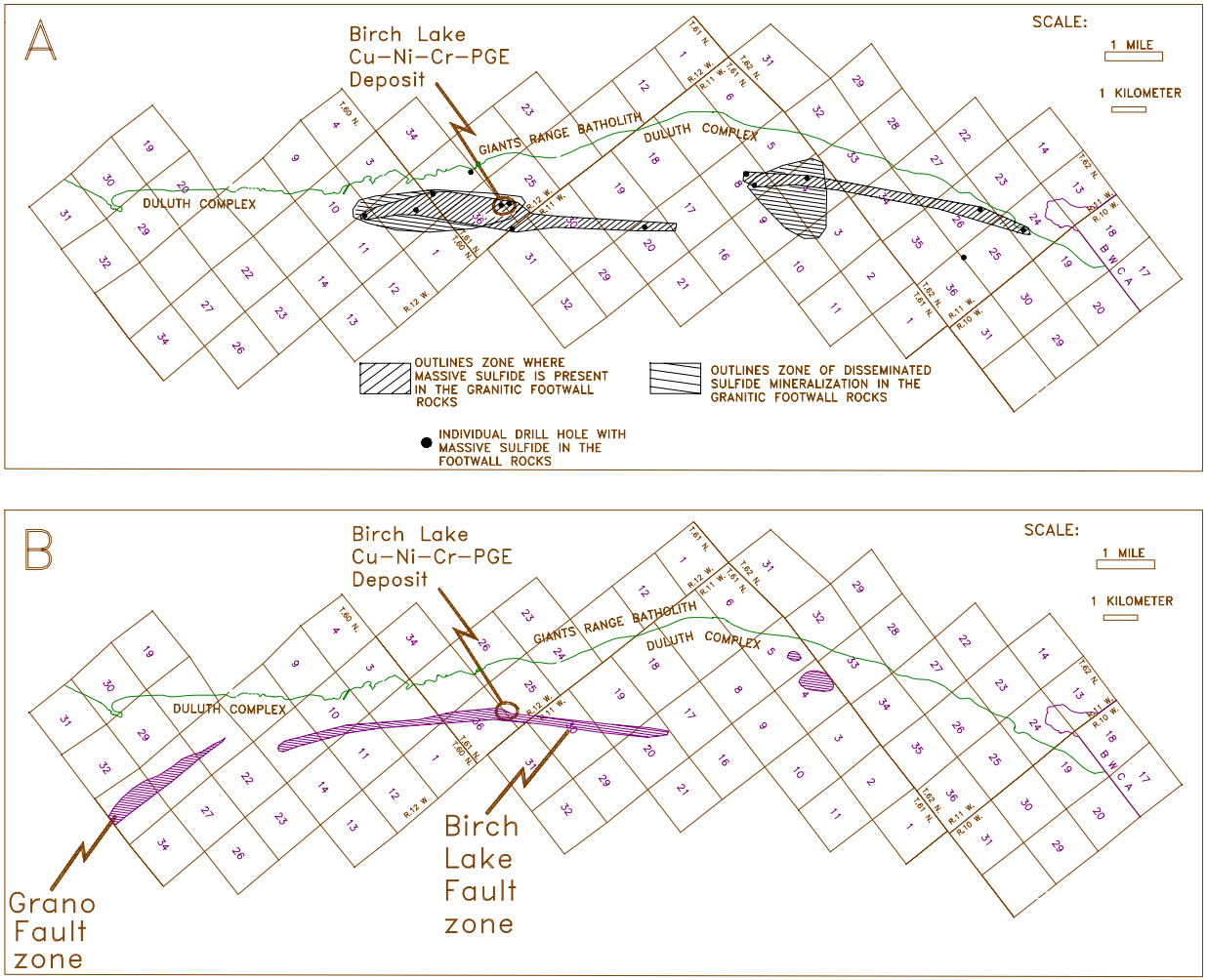

Figure 14. A. Linear distribution of massive sulfides, disseminated sulfides, and copper-rich veins in the Giants Range Batholith footwall; B. Linear distribution of late-stage granitoid and pyroxenitic rocks in the Duluth Complex (after Severson, 1994).